

# Nuclear Shell Model Effective Interactions from Many-Body Perturbation Theory

Zhen Li and Nadezda A. Smirnova

Laboratoire de Physique des Deux Infinis de Bordeaux (LP2I Bordeaux)  
CNRS/IN2P3 - Université de Bordeaux

18/05/2022

# Nuclear Many Body Problem

## A-Body Schrödinger Equation for Nucleus A

$$\hat{H}|\Psi_\alpha\rangle = E_\alpha|\Psi_\alpha\rangle$$
$$\hat{H} = \hat{T} + \hat{V} = \sum_{i=1}^A \frac{\hat{\mathbf{p}}_i^2}{2m} + \sum_{i<j}^A \hat{V}(|\mathbf{r}_i - \mathbf{r}_j|)$$

## Nucleon-Nucleon Interactions

- **Chiral Potentials:** from chiral effective field theory ( $\chi$ EFT), [Machleidt et al., Phys. Rep. 503, 1 \(2011\)](#)
- **Bonn Potentials:** based on meson-exchange models ( $\pi$ ,  $\eta$ ,  $\rho(770)$ ,  $\omega(782)$ ), [Machleidt et al., Phys. Rep. 149, 1 \(1987\)](#), [Machleidt, Phys. Rev. C 63, 024001 \(2001\)](#)
- **Daejeon16 Potential:** based on renormalized chiral potential N<sup>3</sup>LO, fitted to energies of 11 states up to  $A = 16$ , [Shirokov et al., Phys. Lett. B 761, 87 \(2016\)](#)
- **Argonne Potentials:** [Wiringa et al., Phys. Rev. C 51, 38 \(1995\)](#)
- ...

# Nuclear Many Body Problem

## Many-Body Methods for Nuclear System

- ▶ **Monte-Carlo methods (VMC, GFMC, AFDMC, etc.)**
  - J. Carlson et al., Rev. Mod. Phys. 87, 1067 (2015).
- ▶ **Configuration Interaction (CI) methods (SM, NCSM, CC, IM-SRG)**
  - E. Caurier et al., Rev. Mod. Phys. 77, 427 (2005).
  - B. R. Barrett, et al., Prog. Part. Nucl. Phys. 69, 131 (2013).
  - G. Hagen, et al., Rep. Prog. Phys. 77, 096302 (2014).
  - H. Hergert et al., Phys. Rep. 621, 165 (2016).
- ▶ **Self-Consistent Green's Function (SCGF) method**
  - W. H. Dickhoff et al., Prog. Part. Nucl. Phys. 52, 377 (2004).
- ▶ **Many-Body Perturbation Theory (MBPT)**
  - A. Tichai et al., Front. Phys. 8, 164 (2020).
- ▶ **Density Functional Theory (DFT)**
  - M. Bender et al., Rev. Mod. Phys. 75, 121 (2003).
- ▶ **HF, GCM, AMD, ...**

# Shell Model

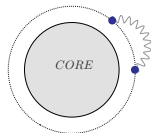
## ► Approximations in Shell Model (Interacting Shell Model, Shell Model with a Core, or Valence Shell Model):

- ① separate the model space into three parts: *Filled Space*, *Valence Space* and *Empty Space*
- ② only consider valence nucleons moving in the *Valence Space*

For example ( $^{18}\text{O}$ ):

- *Filled Space*:  $0s$  and  $0p$  shells, with  $4 + 12 = 16$  nucleons (being inert **core**, double magic nucleus)
- *Valence Space*:  $0d-1s$  shell, with 2 nucleons (the so-called **valence nucleons**)
- *Empty Space*: other shells, without nucleons

	$N$	$d_N$	$\Sigma_N d_N$	Shells	Parity
⋮	⋮	⋮	⋮	⋮	⋮
—————	9	110	440	$0l, 1j, 2h, 3f, 4p$	-
—————	8	90	330	$0k, 1i, 2g, 3d, 4s$	+
—————	7	72	240	$0j, 1h, 2f, 3p$	-
—————	6	56	168	$0i, 1g, 2d, 3s$	+
—————	5	42	112	$0h, 1f, 2p$	-
—————	4	30	70	$0g, 1d, 2s$	+
—————	3	20	40	$0f, 1p$ <i>Empty Space</i>	-
—————	2	12	20	$0d, 1s$ <i>Valence Space</i>	+
—————	1	6	8	$0p$	-
—————	0	2	2	$0s$ <i>Filled Space</i>	+



# Shell Model

▶ **Original  $A$ -Body Problem:**

$$\hat{H}|\Psi_\alpha\rangle = E_\alpha|\Psi_\alpha\rangle$$

▶ **Shell Model:** reduce the  $A$ -body problem to a valence-particle problem inside the valence space

$$\hat{H}_{\text{eff}}^{(v)}|\Psi_\alpha^{\text{P}}\rangle = (E_\alpha - E_c)|\Psi_\alpha^{\text{P}}\rangle$$

- $\hat{H}_{\text{eff}}^{(v)}$ : effective Hamiltonian of valence nucleons in valence space
- $|\Psi_\alpha^{\text{P}}\rangle$ : wavefunctions of valence nucleons in valence space
- $E_\alpha$ : low-lying energies of nucleus  $A$
- $E_c$ : ground state energy of the core nucleus

# Shell Model Effective Hamiltonian

## Effective Hamiltonian of Shell Model

$$H_{\text{eff}} = \sum_{\alpha} \varepsilon_{\alpha} c_{\alpha}^{\dagger} c_{\alpha} + \frac{1}{4} \sum_{\alpha\beta\gamma\delta} \langle \alpha\beta | V_{\text{eff}} | \gamma\delta \rangle c_{\alpha}^{\dagger} c_{\beta}^{\dagger} c_{\delta} c_{\gamma}$$

- $\varepsilon_{\alpha}$ : single-particle energy
- $V_{\text{eff}}$ : effective interaction

# Shell Model Effective Hamiltonian

## Effective Hamiltonian for the Shell Model

$$H_{\text{eff}} = \sum_{\alpha} \varepsilon_{\alpha} c_{\alpha}^{\dagger} c_{\alpha} + \frac{1}{4} \sum_{\alpha\beta\gamma\delta} \langle \alpha\beta | V_{\text{eff}} | \gamma\delta \rangle c_{\alpha}^{\dagger} c_{\beta}^{\dagger} c_{\delta} c_{\gamma}$$

## Effective Interaction $V_{\text{eff}}$

### ► Empirical Effective Interactions:

- $p$ -shell: Cohen-Kurath
- $sd$ -shell: USD, USDB

### ► Microscopic Effective Interactions (from realistic nucleon-nucleon interaction):

- **Many-Body Perturbation Theory (MBPT)**: from 60s, see L. Coraggio et al., *Prog. Part. Nucl. Phys.* 62, 135 (2009), M. Hjorth-Jensen et al., *Phys. Rep.* 261, 125 (1995) and references therein.
- **No-Core Shell Model**: A. F. Lisetskiy et al., *Phys. Rev. C* 78, 044302 (2008), E. Dikmen et al., *Phys. Rev. C* 91, 064301 (2015), N. A. Smirnova et al., *Phys. Rev. C* 100, 054329 (2019).
- **Coupled Cluster**: G. R. Jansen et al., *Phys Rev Lett.* 113, 142502 (2014) and *Phys. Rev. C* 94, 011301 (2016), Sun et al., *Phys. Rev. C* 98, 054320 (2018).
- **In-Medium Similarity Renormalization Group**: S. K. Bogner et al., *Phys Rev Lett.* 113, 142501 (2014), S. R. Stroberg, et al., *Phys Rev Lett.* 118, 032502 (2017).

# Effective Interactions from MBPT ( $\hat{Q}$ -box, or FDT)

Two-body  $\hat{Q}$ -Box<sup>1</sup>: valence-linked irreducible diagrams

$$\langle \alpha\beta | \hat{Q}(\omega) | \gamma\delta \rangle = \langle \text{CORE} | c_\beta c_\alpha H_1(t=0) U_I(0, -\infty) c_\gamma^\dagger c_\delta^\dagger | \text{CORE} \rangle_v,$$

$$H_1 = V - U = \frac{1}{4} \sum_{ijkl} v_{ij,kl} c_i^\dagger c_j^\dagger c_l c_k - \sum_{ij} U_{i,j} c_i^\dagger c_j,$$

$$U_I(0, -\infty) = \lim_{t' \rightarrow -\infty(1-i0^+)} \sum_{n=0}^{\infty} \left( \frac{-i}{\hbar} \right)^n \int_{t'}^{t_1} dt_1 \int_{t'}^{t_2} dt_2 \cdots \int_{t'}^{t_{n-1}} dt_n H_1(t_1) H_1(t_2) \cdots H_1(t_n)$$

Krenciglowa-Kuo Iteration Equation<sup>1</sup>

$$V_{\text{eff}}^{(0)} = \hat{Q}(\omega), \quad V_{\text{eff}}^{(n)} = \hat{Q}(\omega) + \sum_{m=1}^{\infty} \hat{Q}_m(\omega) \left\{ V_{\text{eff}}^{(n-1)} \right\}^m, \quad n \geq 1, \quad \hat{Q}_m(\omega) \equiv \frac{1}{m!} \left[ \frac{d^m \hat{Q}(\omega')}{d\omega'^m} \right]_{\omega'=\omega}$$

Lee-Suzuki Iteration Equation<sup>1</sup>

$$V_{\text{eff}}^{(1)} = \hat{Q}(\omega), \quad V_{\text{eff}}^{(n)} = \left\{ 1 - \hat{Q}_1(\omega) - \sum_{m=2}^{n-1} \hat{Q}_m(\omega) \prod_{k=n-m+1}^{n-1} V_{\text{eff}}^{(k)} \right\}^{-1} \hat{Q}(\omega), \quad n \geq 2$$

<sup>1</sup>T.T.Kuo and E. Osnes, *Folded-diagram theory of the effective interaction in nuclei, atoms and molecules*, Springer-Verlag (1990); E.M. Krenciglowa and T.T.S. Kuo, Nucl. Phys. A 235, 171 (1974); K. Suzuki and S.Y. Lee, Prog. Theor. Phys. 64, 2091 (1980); L. Coraggio et al., Prog. Part. Nucl. Phys. 62, 135 (2009), M. Hjorth-Jensen et al., Phys. Rep. 261, 125 (1995).



# Effective Interactions from MBPT

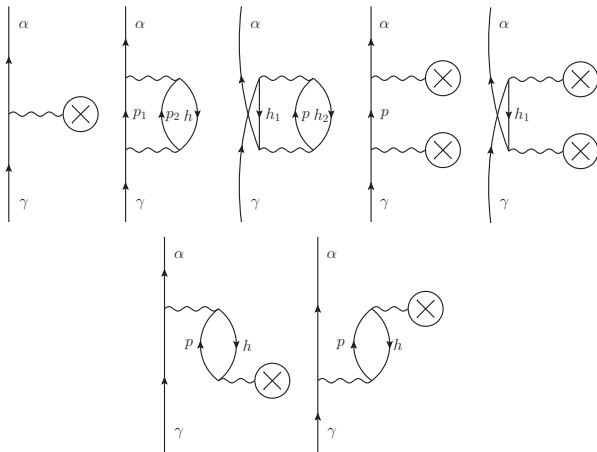


Figure: One-body  $\hat{Q}$ -box diagrams up to second order.

# Effective Interactions from MBPT

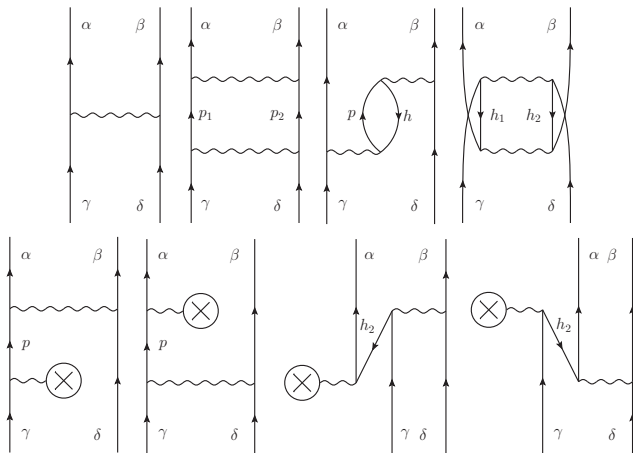


Figure: Two-body  $\hat{Q}$ -box diagrams up to second order.

# Effective Interactions from MBPT

## ▶ Diagram Expressions:

$$\begin{array}{|c|} \alpha \\ \hline \text{---} \\ \gamma \end{array} \begin{array}{|c|} \beta \\ \hline \text{---} \\ \delta \end{array} = \langle \alpha\beta | V | \gamma\delta \rangle, \quad \begin{array}{|c|} \alpha \\ \hline \text{---} \\ p_1 \\ \hline \text{---} \\ p_2 \\ \hline \text{---} \\ \gamma \end{array} \begin{array}{|c|} \beta \\ \hline \text{---} \\ p_2 \\ \hline \text{---} \\ p_1 \\ \hline \text{---} \\ \delta \end{array} = \frac{1}{2} \sum_{p_1 p_2} \frac{\langle \alpha\beta | V | p_1 p_2 \rangle \langle p_1 p_2 | V | \gamma\delta \rangle}{\epsilon_\gamma + \epsilon_\delta - \epsilon_{p_1} - \epsilon_{p_2}}, \dots$$

## ▶ $(V-U)$ -insertion diagrams:

$$\begin{array}{|c|} \alpha \\ \hline \text{---} \otimes \\ \gamma \end{array} \equiv \begin{array}{|c|} \alpha \\ \hline \text{---} \circ \\ \gamma \end{array} + \begin{array}{|c|} \alpha \\ \hline \text{---} \times \\ \gamma \end{array} = \sum_h \langle \alpha h | V | \gamma h \rangle + \langle \alpha | (-U) | \gamma \rangle, \dots$$

- $(V-U)$ -insertion diagrams are usually neglected in most applications, assuming that the single-particle wavefunctions of HO and HF are the same;
- $\hbar\omega$  dependence of effective interaction will present without including  $(V-U)$ -insertion diagrams order by order<sup>1</sup>.

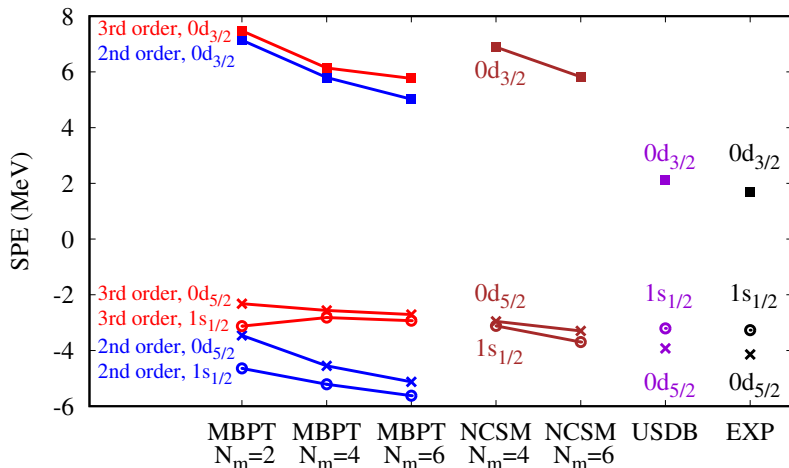
<sup>1</sup>L. Coraggio, et al., Annals of Physics 327, 2125 (2012).

- ▶ **Our work:** we have developed a m-scheme Fortran code that allows us to calculate shell model effective Hamiltonians (single-particle energies + effective interactions) in the framework of MBPT (or the so-called  $\hat{Q}$ -box method, folded-diagram theory) with  $(V-U)$ -insertion diagrams order by order.
- ▶ **Preliminary** results: *sd*-shell single-particle energies and effective interactions were derived from realistic interaction Daejeon16 (DJ16) with up to third order diagrams.

*sd*-shell single-particle energies

# *sd*-shell results, single-particle energies

## ► Theoretical Single Particle Energy (SPE) from DJ16:



NCSM: N. A. Smirnova, et al., Phys. Rev. C 100, 5 (2019); I. J. Shin, et al., to be published;

EXP: N. Schwierz, et al., arXiv:0709.3525;

USDB: B.A. Brown et al., Phys. Rev. C 74, 034315 (2006).

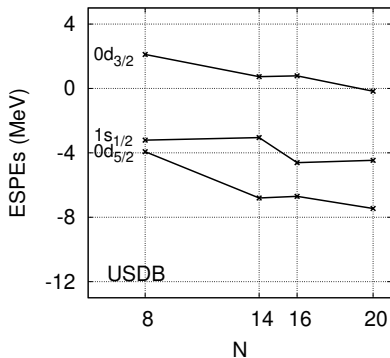
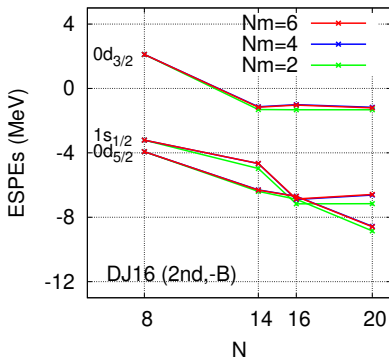
*sd*-shell effective interactions

# $sd$ -shell results, effective interactions

Effective Single-Particle Energies (ESPEs)<sup>1</sup>: single particle energy in the mean field approximation

$$\tilde{\epsilon}_k^\rho = \epsilon_k^\rho + \sum_{k'\rho'} V_{kk'}^{\rho\rho'} n_{k'}^{\rho'}, \quad V_{kk'}^{\rho\rho'} = \frac{\sum_J \langle k_\rho k'_{\rho'} | V | k_\rho k'_{\rho'} \rangle_J (2J+1)}{\sum_J (2J+1)}$$

► Neutron ESPEs of Oxygen isotopes at sub-shell closures  $N = 8, 14, 16, 20$  derived from DJ16 at 2nd order, without  $(V-U)$ -insertion diagrams



<sup>1</sup>R. K. Bansal and J. B. French, Phys. Lett. 11, 145 (1964), T. Otsuka et al., Prog. Part. Nucl. Phys. 47, 319 (2001), N. A. Smirnova et al., Phys. Lett. B 686, 109 (2010)

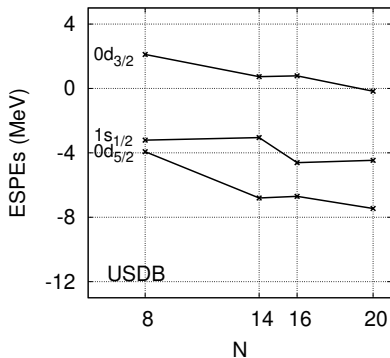
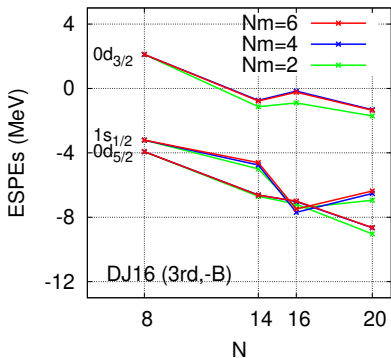


# $sd$ -shell results, effective interactions

Effective Single-Particle Energies (ESPEs)<sup>1</sup>: single particle energy in the mean field approximation

$$\tilde{\epsilon}_k^\rho = \epsilon_k^\rho + \sum_{k'\rho'} V_{kk'}^{\rho\rho'} n_{k'}^{\rho'}, \quad V_{kk'}^{\rho\rho'} = \frac{\sum_J \langle k_\rho k'_{\rho'} | V | k_\rho k'_{\rho'} \rangle_J (2J+1)}{\sum_J (2J+1)}$$

► Neutron ESPEs of Oxygen isotopes at sub-shell closures  $N = 8, 14, 16, 20$  derived from DJ16 at 3rd order, without (V-U)-insertion diagrams



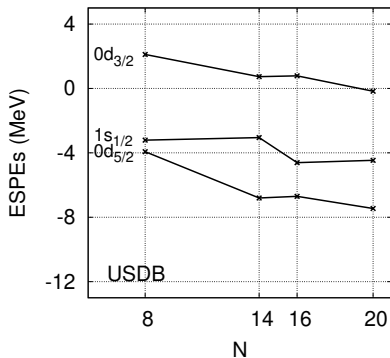
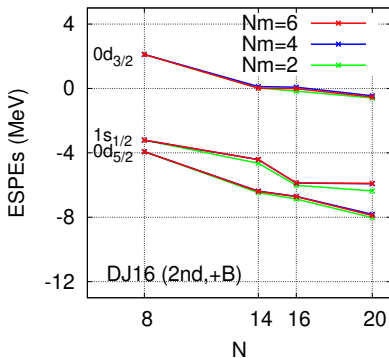
<sup>1</sup>R. K. Bansal and J. B. French, Phys. Lett. 11, 145 (1964), T. Otsuka et al., Prog. Part. Nucl. Phys. 47, 319 (2001), N. A. Smirnova et al., Phys. Lett. B 686, 109 (2010)

# $sd$ -shell results, effective interactions

Effective Single-Particle Energies (ESPEs)<sup>1</sup>: single particle energy in the mean field approximation

$$\tilde{\epsilon}_k^\rho = \epsilon_k^\rho + \sum_{k'\rho'} V_{kk'}^{\rho\rho'} n_{k'}^{\rho'}, \quad V_{kk'}^{\rho\rho'} = \frac{\sum_J \langle k_\rho k'_{\rho'} | V | k_\rho k'_{\rho'} \rangle_J (2J+1)}{\sum_J (2J+1)}$$

► Neutron ESPEs of Oxygen isotopes at sub-shell closures  $N = 8, 14, 16, 20$  derived from DJ16 at 2nd order with  $(V-U)$ -insertion diagrams



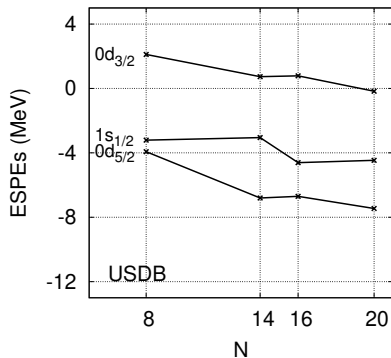
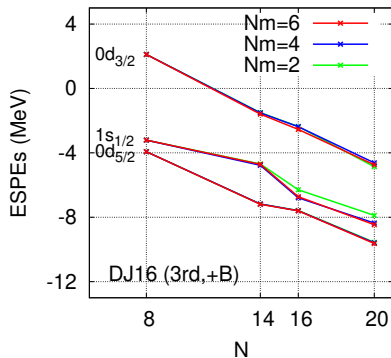
<sup>1</sup>R. K. Bansal and J. B. French, Phys. Lett. 11, 145 (1964), T. Otsuka et al., Prog. Part. Nucl. Phys. 47, 319 (2001), N. A. Smirnova et al., Phys. Lett. B 686, 109 (2010)

# $sd$ -shell results, effective interactions

Effective Single-Particle Energies (ESPEs)<sup>1</sup>: single particle energy in the mean field approximation

$$\tilde{\epsilon}_k^\rho = \epsilon_k^\rho + \sum_{k'\rho'} V_{kk'}^{\rho\rho'} n_{k'}^{\rho'}, \quad V_{kk'}^{\rho\rho'} = \frac{\sum_J \langle k_\rho k'_{\rho'} | V | k_\rho k'_{\rho'} \rangle_J (2J+1)}{\sum_J (2J+1)}$$

► Neutron ESPEs of Oxygen isotopes at sub-shell closures  $N = 8, 14, 16, 20$  derived from DJ16 at 3rd order with  $(V-U)$ -insertion diagrams

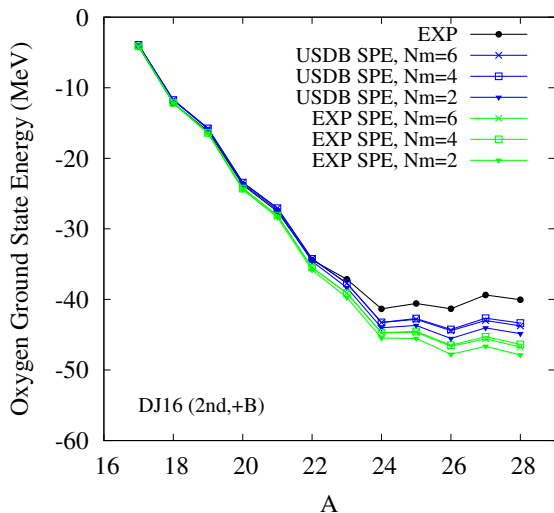


<sup>1</sup>R. K. Bansal and J. B. French, Phys. Lett. 11, 145 (1964), T. Otsuka et al., Prog. Part. Nucl. Phys. 47, 319 (2001), N. A. Smirnova et al., Phys. Lett. B 686, 109 (2010)

**Some *sd*-shell nuclei calculations with the  
derived effective Hamiltonians  
(single-particle energies + effective  
interactions).**

# *sd*-shell results, including (*V-U*)-insertion diagrams order by order

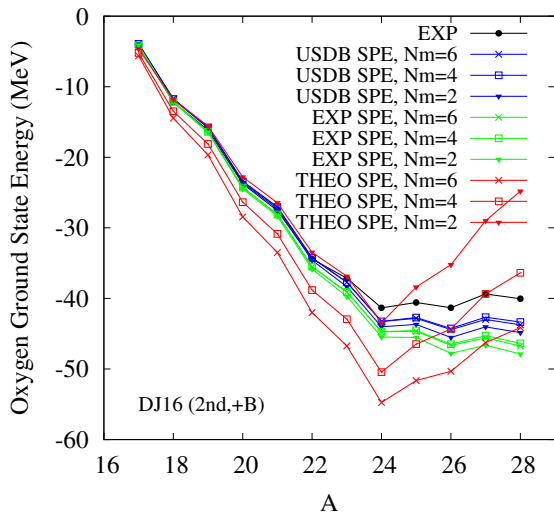
## ► Binding Energies<sup>1</sup> of <sup>A</sup>O relative to <sup>16</sup>O at 2nd order:



<sup>1</sup>All the shell model calculations are performed with the code Antoine: E. Caurier, et al., Rev. Mod. Phys. 77, 2 (2005).

# *sd*-shell results, including (*V-U*)-insertion diagrams order by order

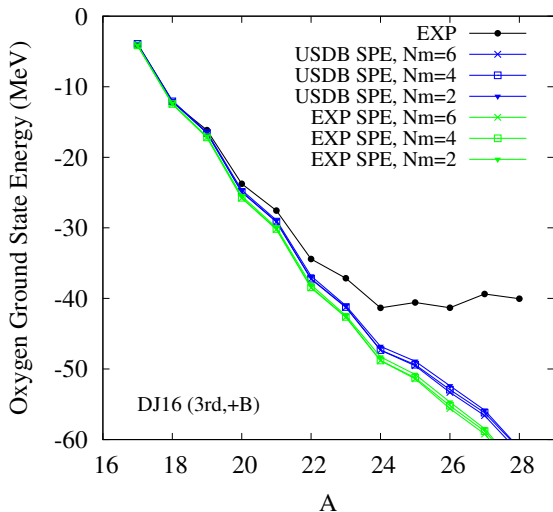
## ► Binding Energies<sup>1</sup> of <sup>A</sup>O relative to <sup>16</sup>O at 2nd order:



<sup>1</sup>All the shell model calculations are performed with the code Antoine: E. Caurier, et al., Rev. Mod. Phys. 77, 2 (2005).

# *sd*-shell results, including (*V-U*)-insertion diagrams order by order

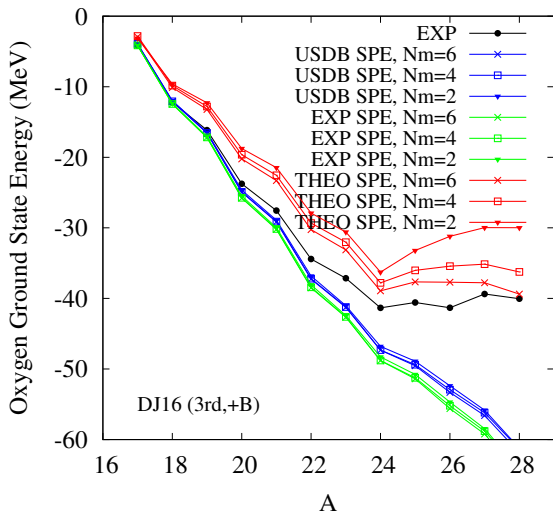
## ► Binding Energies<sup>1</sup> of <sup>A</sup>O relative to <sup>16</sup>O at 3rd order:



<sup>1</sup>All the shell model calculations are performed with the code Antoine: E. Caurier, et al., Rev. Mod. Phys. 77, 2 (2005).

# *sd*-shell results, including (*V-U*)-insertion diagrams order by order

## ► Binding Energies<sup>1</sup> of <sup>A</sup>O relative to <sup>16</sup>O at 3rd order:

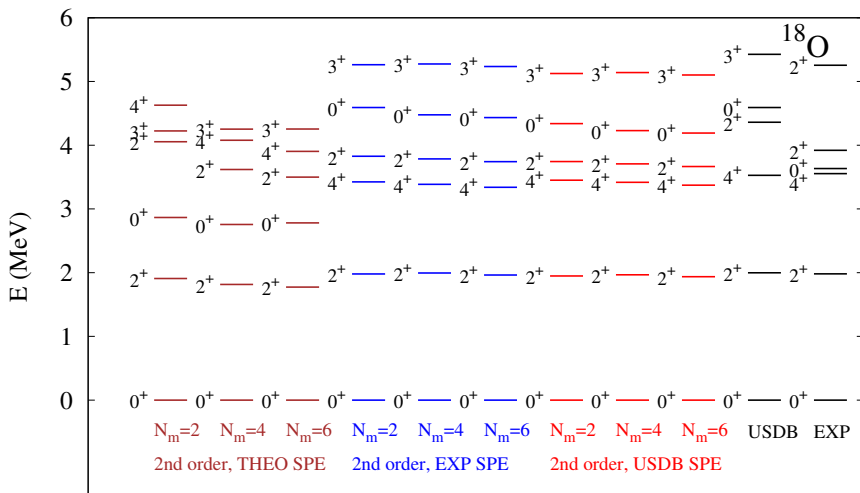


<sup>1</sup>All the shell model calculations are performed with the code Antoine: E. Caurier, et al., Rev. Mod. Phys. 77, 2 (2005).



# *sd*-shell results, including (*V-U*)-insertion diagrams order by order

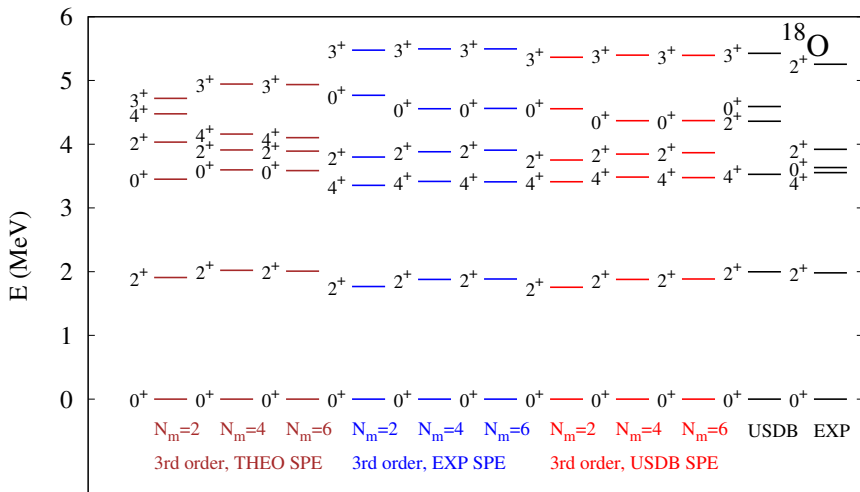
## ► Six lowest positive-parity states<sup>1</sup> of <sup>18</sup>O at 2nd order:



<sup>1</sup>All the shell model calculations are performed with the code Antoine: E. Caurier, et al., Rev. Mod. Phys. 77, 2 (2005).

# *sd*-shell results, including (*V-U*)-insertion diagrams order by order

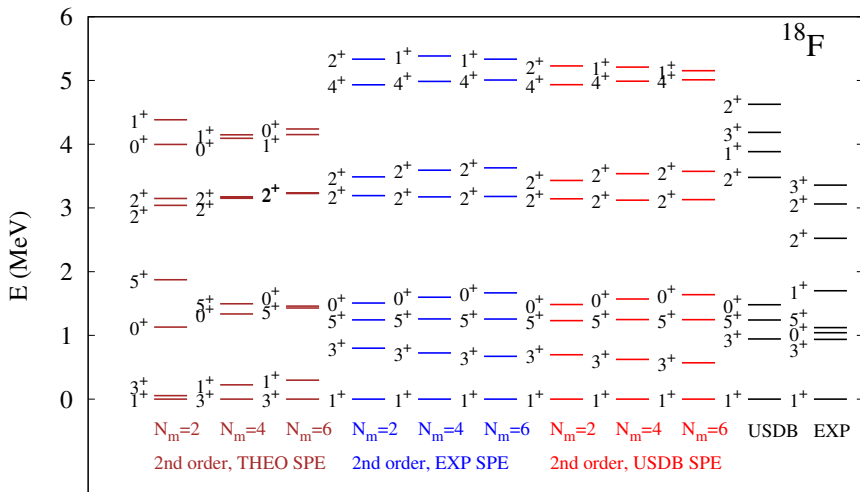
## ► Six lowest positive-parity states<sup>1</sup> of <sup>18</sup>O at 3rd order:



<sup>1</sup>All the shell model calculations are performed with the code Antoine: E. Caurier, et al., Rev. Mod. Phys. 77, 2 (2005).

# *sd*-shell results, including (*V-U*)-insertion diagrams order by order

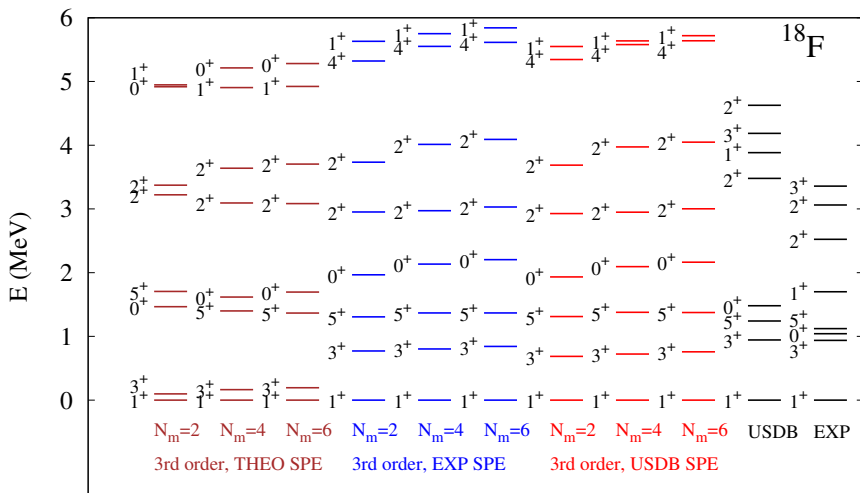
## ► Eight lowest positive-parity states<sup>1</sup> of <sup>18</sup>F at 2nd order:



<sup>1</sup>All the shell model calculations are performed with the code Antoine: E. Caurier, et al., Rev. Mod. Phys. 77, 2 (2005).

# *sd*-shell results, including (*V-U*)-insertion diagrams order by order

## ► Eight lowest positive-parity states<sup>1</sup> of <sup>18</sup>F at 3rd order:



<sup>1</sup>All the shell model calculations are performed with the code Antoine: E. Caurier, et al., Rev. Mod. Phys. 77, 2 (2005).

# *sd*-shell results, including (*V-U*)-insertion diagrams order by order

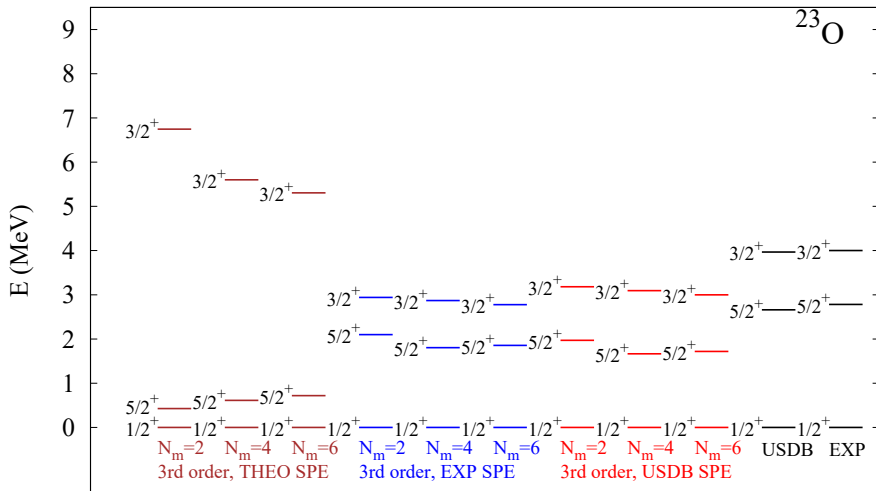
## ▶ Three lowest positive-parity states<sup>1</sup> of <sup>23</sup>O at 2nd order:



<sup>1</sup>All the shell model calculations are performed with the code Antoine: E. Caurier, et al., Rev. Mod. Phys. 77, 2 (2005).

# *sd*-shell results, including (*V-U*)-insertion diagrams order by order

► Three lowest positive-parity states<sup>1</sup> of <sup>23</sup>O at 3rd order:



<sup>1</sup>All the shell model calculations are performed with the code Antoine: E. Caurier, et al., Rev. Mod. Phys. 77, 2 (2005).

# Summary

- ▶ A Fortran code to calculate effective Hamiltonian was developed in the framework of MBPT.
- ▶ *sd*-shell single-particle energies and effective interactions are derived from DJ16 using MBPT with up to third order diagrams.
- ▶ The single-particle energies derived at third order are similar to the NCSM results.
- ▶ The centroids of the derived effective interactions are too attractive, which results in too small sub-shell gaps. This deficiency leads to overbinding problems in the description of neutron-rich nuclei, and poor spectroscopy of nuclei in the vicinity of sub-shell closures.
- ▶ The ( $V-U$ )-insertion diagrams can improve the deficient centroids.
- ▶ Third order results give better spectroscopy of nuclei but worse binding energies of neutron-rich nuclei compared to second order results. Therefore, higher order diagrams are expected to give some corrections.

**Thank you for your attention**



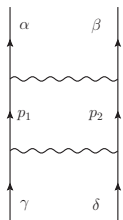
$$U = \sum_{i=1}^A u_i = \sum_{i=1}^A \left\{ \frac{1}{2} m \omega^2 r_i^2 + \Delta \right\}$$

$$\varepsilon_\alpha = \left( 2n + l + \frac{3}{2} \right) \hbar \omega + \Delta$$

The diagrammatic equation shows the interaction between two particles,  $\alpha$  and  $\gamma$ . On the left, a vertical line for  $\alpha$  and a vertical line for  $\gamma$  are connected by a wavy line with a circle containing an 'X' (representing the potential  $-U$ ). This is shown to be equivalent to the sum of two terms: 1) a wavy line with a circle containing 'h' (representing the potential  $V$ ), and 2) a wavy line with an 'X' (representing the potential  $-U$ ). The equation is then equated to a summation over states  $h$  of the matrix elements  $\langle \alpha h | V | \gamma h \rangle + \langle \alpha | (-U) | \gamma \rangle$ .

$$\text{Diagram} \equiv \text{Diagram}_1 + \text{Diagram}_2 = \sum_h \langle \alpha h | V | \gamma h \rangle + \langle \alpha | (-U) | \gamma \rangle$$

# Backup


$$= \frac{1}{2} \sum_{p_1 p_2} \frac{\langle \alpha \beta | V | p_1 p_2 \rangle \langle p_1 p_2 | V | \gamma \delta \rangle}{\epsilon_\gamma + \epsilon_\delta - \epsilon_{p_1} - \epsilon_{p_2}}$$

$$|N_\gamma + N_\delta - N_{p_1} - N_{p_2}| \leq N_{\max}$$

$$N = 2n + l$$